

# Alloy composition and electronic structure of $\text{Cd}_{1-x}\text{Zn}_x\text{Te}$ by surface photovoltage spectroscopy

Jihua Yang, Y. Zidon, and Yoram Shapira<sup>a)</sup>

*Department of Physical Electronics, Tel-Aviv University, Ramat-Aviv 69978, Israel*

(Received 29 January 2001; accepted for publication 15 October 2001)

The alloy composition of a  $\text{Cd}_{1-x}\text{Zn}_x\text{Te}$ (111) sample and its spatial homogeneity have been determined by surface photovoltage spectroscopy (SPS) and compared to conventional energy dispersive x-ray spectroscopy measurements. Experimental improvements of the former technique yield a contactless, surface sensitive, and highly accurate spectral resolution of the band gap (error < 4 meV) and consequently of the Zn concentration (error < 0.6% in comparison with the latter technique). In addition, SPS is capable of determining the face and type of the  $\text{Cd}_{1-x}\text{Zn}_x\text{Te}$  as well as identifying gap states at its surface. The electronic structure has been investigated in comparison with *n*-CdTe(111), before and after various surface chemical treatments. An acceptor surface state has been observed at 1.21 eV below the conduction band edge and attributed to  $\text{TeO}_2$ . A donor surface state (with a lower concentration relative to the corresponding state in CdTe) associated with Cd atom displacement has been found at 1.42 eV above the valence band maximum. A chemically induced surface state at 0.72 eV below the conduction band edge may be due to Zn vacancies, as supported by x-ray photoelectron spectroscopy measurements. © 2002 American Institute of Physics. [DOI: 10.1063/1.1425071]

## I. INTRODUCTION

CdTe and its ternary alloy  $\text{Cd}_{1-x}\text{Zn}_x\text{Te}$  are important semiconductor materials that are used in solar cells, x-ray detectors and other optoelectronic devices.<sup>1-3</sup> Due to their chemical and structural compatibility, they are also the material of choice as substrates for growing epitaxial layers of HgCdTe, a useful IR detecting material in the 8–12  $\mu\text{m}$  infrared range. The introduction of Zn into CdTe makes the lattice of  $\text{Cd}_{1-x}\text{Zn}_x\text{Te}$  tunable, by adjusting the Cd/Zn ratio, hence, a better lattice-matched substrate for the growth of the HgCdTe epitaxial layer may be expected.<sup>4</sup> Furthermore, the designable semiconductor band gap is obviously helpful for controlling the resistivity as well as the valence and conduction band alignment at the semiconductor interface.

The control and monitoring of the Zn concentration,  $x$ , especially at the surface, is crucial for obtaining a  $\text{Cd}_{1-x}\text{Zn}_x\text{Te}$  alloy with the required lattice parameter for matching HgCdTe. Also, it is an important consideration for its use as a detector material. Besides direct determination from the measurement of the lattice parameter,  $x$  can be obtained by the determination of the alloy band gap. Using room temperature photoreflectance and lattice parameter measurements, Tobin *et al.* observed a relation between the band gap and  $x$ :<sup>5</sup>

$$E_g = 1.5045 + 0.631x + 0.128x^2, \quad (1)$$

where  $E_g$  is the band gap of the alloy, in electron volts, and 1.5045 eV is the band gap of CdTe.

From Eq. (1), Zn concentrations of  $x$  between 0.06 and 0.07 yield band gaps of  $E_g$  between 1.5428 and 1.5493 eV, respectively, a difference of less than 7 meV. Therefore, for such  $x$  values, the measured band gap should be accurate to within several milli-electron volts, for errors less than  $\pm 0.01$  in  $x$ . Hence, if optical techniques are to be used, both the incident light source and the detector must have high spectral resolution. Several techniques, e.g., photoreflectance and low temperature photoluminescence have been used to determine the CdZnTe band gap and thus  $x$ .<sup>5</sup>

We have measured the band gap of a  $\text{Cd}_{1-x}\text{Zn}_x\text{Te}$ (111) samples and determined this alloy Zn concentration with high accuracy using surface photovoltage spectroscopy (SPS).<sup>6</sup> It has been assumed that the band gap values measured by SPS could be obtained with an accuracy of about 0.1–0.2 eV, but we have improved the technique resolution by introducing a band gap measurement methodology, i.e., the band gap reference point is selected at the second knee of the band gap related transition, where the surface photovoltage reaches saturation as well as by using extremely slow and very small-stepped scans (see Sec. III A). The high accuracy has been proven by comparative measurements on the same sample using SPS and energy dispersive x-ray spectroscopy (EDS). Measuring at eight different surface positions, the homogeneity of the Zn concentration has been examined. Furthermore, it is important to characterize and control the surface electronic structure and chemical composition of the substrate for epitaxial layer growth and device performance.<sup>7-9</sup> In comparison with the Cd-rich (i.e., the Cd crystallographic) surface of *n*-CdTe(111), we have studied and assigned several transitions at the alloy surface to chemical species using SPS and x-ray photoelectron spectroscopy (XPS).

<sup>a)</sup> Author to whom correspondence should be addressed; electronic mail: shapira@eng.tau.ac.il

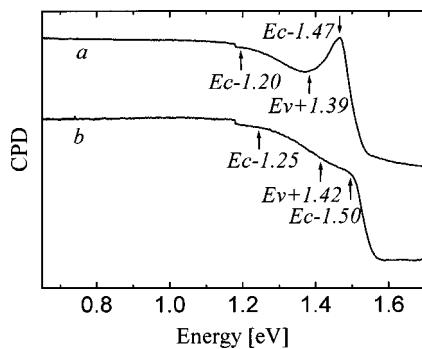


FIG. 1. SPV curves as a function of illumination energy measured at Cd-rich surfaces of a CdTe sample (a) and a  $\text{Cd}_{1-x}\text{Zn}_x\text{Te}$  sample (b). Important transitions are marked by arrows (some are more easily detected if magnified). The spectra are vertically shifted for clarity.

## II. EXPERIMENT

The CdTe sample and the  $\text{Cd}_{1-x}\text{Zn}_x\text{Te}$  samples were provided by Imarad Imaging Systems Ltd, Israel. The Cd-rich surfaces of CdTe and  $\text{Cd}_{1-x}\text{Zn}_x\text{Te}$  were identified by a standard etching test.<sup>10</sup> All the surface photovoltage (SPV) spectra of CdTe and  $\text{Cd}_{1-x}\text{Zn}_x\text{Te}$  were measured in ambient temperature using a Kelvin probe arrangement (Delta-Phi Elektronik, Germany). A spectrometer with a double monochromator (McPherson Inc., USA) provided monochromatic incident light with a resolution about 0.18 nm. This yields an energy error of less than 4 meV for the measured band gap values of the  $\text{Cd}_{1-x}\text{Zn}_x\text{Te}$  samples. In order to obtain an accurate value of the band gap, the monochromator was scanned with 0.2 nm (0.4 meV) steps and a 10 s dwell time at each step. This procedure provided a sufficiently equilibrated signal response at every sampled wavelength to ensure a minimal experimental error. In the study of the surface states, the SPS spectra were taken from 2000 to 450 nm, with 2.0 nm steps and 1 s dwell time.

To assign the observed transitions to chemical species, various surface chemical treatments were performed on the same  $\text{Cd}_{1-x}\text{Zn}_x\text{Te}$  sample. SPS was measured immediately after 1 min etching in 1%  $\text{Br}_2/\text{CH}_3\text{OH}$ ;<sup>11</sup> HCl; 5M KOH,<sup>12</sup> and 5M KOH+3 M NaCl solutions, respectively. Unless otherwise noted, the etchings were carried out at room temperature.

XPS measurements were performed in an UHV system ( $2 \times 10^{-10}$  Torr base pressure) using a 5600 Multi-Technique System (PHI, USA). The samples were irradiated with an Al  $K\alpha$  monochromated source (1486.6 eV) and the photoelectrons were analyzed by a hemispherical analyzer using a slit aperture of 0.8 mm in diameter.

## III. RESULTS AND DISCUSSION

### A. Determination of $\text{Cd}_{1-x}\text{Zn}_x\text{Te}$ alloy composition

Figure 1 shows the SPV spectra of the Cd-rich surfaces of a CdTe sample [curve (a)] and a  $\text{Cd}_{1-x}\text{Zn}_x\text{Te}$  sample [curve (b)]. The band gap-related transition of the  $\text{Cd}_{1-x}\text{Zn}_x\text{Te}$  is blueshifted in comparison with the CdTe due to the introduction of Zn. Since ZnTe has a larger band gap (2.263 eV) than CdTe (1.504 eV), the  $\text{Cd}_{1-x}\text{Zn}_x\text{Te}$  alloy

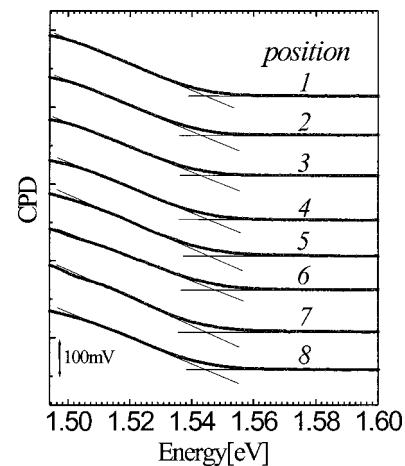


FIG. 2. SPV curves of the  $\text{Cd}_{1-x}\text{Zn}_x\text{Te}$  sample of Fig. 1(b) at eight different surface positions (about 3 mm apart) and associated band gap measurements. The intersection point of the tangents is the suggested band gap position. The spectra are vertically shifted for clarity.

band gap increases with  $x$ . All the features below the band gap values arise from subband gap transitions. The physical mechanisms of the latter transitions are discussed later.

Conventionally, the band gap is estimated using the onset of the slope change (knee) in the SPV curve,<sup>13,14</sup> signifying the start of the band gap response, or the maximum of the SPV derivative, which is the midpoint between the knees.<sup>15</sup> The energy position is usually found by the tangent intersection and is limited in accuracy to about 0.1–0.2 eV. SPV spectral shape follows that of the absorption spectrum which is known to have an  $\alpha \sim (h\nu - E_g)^n$  behavior with  $n = 1/2$  or 2 for direct or indirect semiconductor, respectively. The band gap can thus also be obtained by the extrapolation of a  $(\text{SPV})^2$  or  $(\text{SPV})^{1/2}$  curve.<sup>16</sup>

Since SPS is in fact an electro-optical method, the details of the density of states (DOS) at the conduction band edge of the semiconductor have to be considered. The ubiquitous band tail at the bottom of the conduction band as well as possible states or minibands next to it may blur the true position of the band gap. The low concentration of states at those points is the cause of the slope change of the SPV curve. Only the energy at which the DOS reaches its parabolic dependence is a true indication of the band gap and in retrospect, this is obvious in many studies [including curve (a) in Fig. 1].<sup>17–19</sup> Thus, a better point of reference should be the succeeding knee, where the SPV response reaches saturation after the transition. The saturation is used as a baseline for the tangent while it may be absent in cases of high carrier surface recombination.<sup>14</sup>

To obtain the band gap more accurately, we have also chosen better experimental conditions. We have used a double monochromator (to avoid stray light and have a narrower bandwidth), which was scanned with a 10 s dwell time (to have a sufficiently equilibrated response) and an increment of 0.2 nm ( $\sim 0.4$  meV at the scan range of 830–775 nm) to ensure a minimum experimental error. The scan range was selected as indicated by curve (b) in Fig. 1.

Figure 2 shows the measured SPV curves of the  $\text{Cd}_{1-x}\text{Zn}_x\text{Te}$  sample at eight different surface positions

TABLE I. Band gap and Zn concentration  $x$  of the  $\text{Cd}_{1-x}\text{Zn}_x\text{Te}$  determined by SPS, at eight different surface positions.  $\Delta E_g$  is the band gap increase, due to Zn introduction, relative to CdTe.

Position measured	Band gap ( $E_g$ ) (eV)	$\Delta E_g$ (eV)	$x \pm 0.006$
1	1.545	0.041	0.064
2	1.543	0.039	0.061
3	1.543	0.039	0.061
4	1.545	0.041	0.064
5	1.544	0.040	0.063
6	1.547	0.043	0.067
7	1.544	0.040	0.063
8	1.545	0.041	0.064

(about 3 mm distant from each other) for band gap evaluation. The suggested method of determining the intersection point of the tangents to read the band gap value is also illustrated. From the band gap position, the Zn concentration was calculated using Eq. (1) and is shown in Table I. An averaged  $x$  value of  $0.063 \pm 0.006$  is obtained. The largest  $x$  discrepancy among different measured positions is 0.006, probably due to Zn segregation effects in the ingot. Therefore, in the investigation range, the current sample has a rather homogeneous  $x$  distribution.

To examine the accuracy of this improved SPS technique, as well as of the proposed method for band gap determination, we have measured a reference CdZnTe sample using our technique and compared the results with EDS measurements (accuracy of  $\sim 0.5\%$ ) taken at the same points on the sample. Naturally, the EDS measurements are taken with very small spot size relative to SPS, which averages the signal over the probe size (2.5 mm in diameter). Also, SPS is more surface sensitive (limited to the space charge region width, in our case within  $0.1 \mu\text{m}$ ) while EDS averages the signal over a depth of about  $1 \mu\text{m}$ . Figure 3 shows the SPV curves of the sample at nine different points on the reference sample. Table II gives the measured band gap values and compares  $x$  determined by SPS and EDS measurements. Although at positions 3 and 8, the discrepancy is somewhat

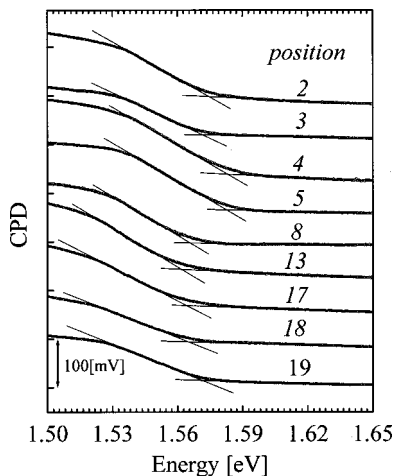


FIG. 3. SPV curves as a function of illumination energy and associated band gap measurements at nine different positions on a reference CdZnTe sample. The spectra are vertically shifted for clarity.

TABLE II. Zn concentration  $x$  of a CdZnTe sample as determined by SPS and EDS at nine different surface positions.

Position measured	SPS		EDS
	Band gap (eV)	$x \pm 0.006$	$x \pm 0.005$
2	1.575	0.109	0.118
3	1.571	0.103	0.119
4	1.583	0.0121	0.121
5	1.583	0.121	0.123
8	1.566	0.096	0.108
13	1.562	0.090	0.096
17	1.564	0.093	0.097
18	1.563	0.091	0.092
19	1.571	0.103	0.097

large (about 1.6% and 1.2%, respectively), the other seven examined points have a good agreement with a discrepancy of  $< 1\%$ . This is also shown in Fig. 4, which describes the measurement positions as well as the results of both techniques with their associated error bars.

Since the band gap of  $\text{Cd}_{1-x}\text{Zn}_x\text{Te}$  with low Zn concentration can be obtained with an accuracy of  $< 4 \text{ meV}$  by SPS, the Zn concentration can be determined with an error  $< 0.6\%$ . Thus, this technique yields far better accuracies than are usually reported by SPS users. Considering its operation simplicity, surface sensitivity, and its *in situ* applicability, this technique can be used as an effective analytical tool for the highly accurate determination of CdZnTe alloy composition and most probably as a universal tool for other alloys.

**B. Surface states of CdTe and  $\text{Cd}_{0.937}\text{Zn}_{0.063}\text{Te}$**

Curve (a) in Fig. 1 shows that the contact potential difference (CPD) of the CdTe sample decreases abruptly with an incident photon energy above 1.47 eV, signifying that the CdTe sample is *n* type. The transition energy is shifted from the band gap energy (1.5045 eV) by about 35 meV (close to  $kT$ ) reflecting the band tail effect. Similar considerations apply to CdZnTe [curve (b)], in which the band tail effect starts at about 1.50 eV.

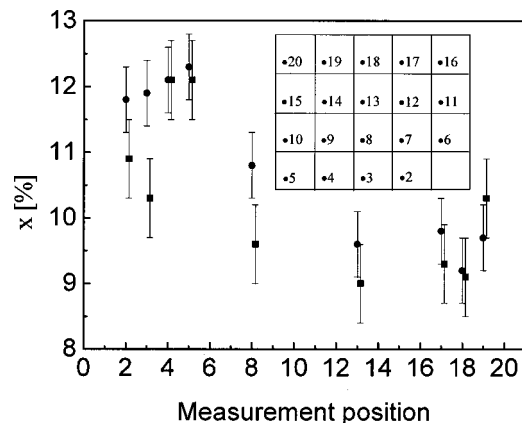


FIG. 4. SPS (full squares) and EDS (full circles) measurements of Zn concentration  $x$  (%) at the same positions on the reference CdZnTe sample of Fig. 3. The positions are slightly shifted for clarity. Inset shows the position of the measurement points on the sample.

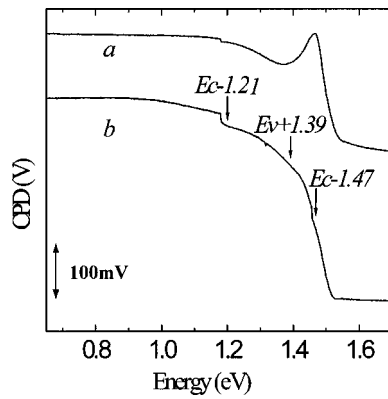


FIG. 5. SPV curves of Cd-rich surfaces of CdTe before (a) and after (b) etching by 1%  $\text{Br}_2/\text{CH}_3\text{OH}$ . The spectra are vertically shifted for clarity.

Two obvious subband gap transitions are observed at  $1.21 \pm 0.05$  eV ( $E_1$ ) and  $\sim 1.39 \pm 0.05$  eV ( $E_2$ ), respectively [The jump at 1.18 eV is a filter changing effect. It should be noted that it has no effect on the accuracy of the spectroscopy. The jump does not evolve from the light source spectrum but rather from stray light effects that even a double monochromator arrangement cannot entirely eliminate. However, the accuracy of the observed transitions ( $\sim 0.05$  eV) is lower than that of the band gap measurements]. The transition at  $E_1$  has a negative slope change and thus is characteristic of electron transition from an occupied acceptor surface state at 1.21 eV below the conduction band minimum (CBM) to the CBM. The other transition at  $E_2$  shows a positive CPD slope change, indicating photoexcitation from the valence band maximum (VBM) to an unoccupied donor surface state situated  $\sim 1.39$  eV above the VBM.

In a previous article,<sup>20</sup> Burstein *et al.* have shown that SPS can distinguish between the electronic structures of CdTe Cd-rich and Te-rich surfaces. They identified two kinds of surface states on the Cd-rich surface of  $p$ -CdTe. One kind was an acceptor state at 1.17 eV below the CBM and is attributed to  $\text{TeO}_2$ -CdTe interaction. The other kind was due to Cd atom displacement (i.e., Cd atom perturbation from its normal position on the surface by the preferential oxygen adsorption on Te surface sites). These states are found to be unoccupied and situated at 1.11 and 1.33 eV above the VBM, respectively. By comparison, we conclude that the transitions at  $E_1$  and  $E_2$  of our  $n$ -CdTe are also due to the  $\text{TeO}_2$ -CdTe interaction and the Cd atom displacement, respectively.

The same CdTe sample was etched using  $\text{Br}_2/\text{CH}_3\text{OH}$  solution, which would leave either Cd-rich or Te-rich surfaces with a thick Cd-depleted  $\text{TeO}_2$  layer.<sup>11</sup> This should make the SPV signal due to the  $\text{TeO}_2$ -CdTe interaction surface state become dominant while that from the Cd atom displacement weaker.<sup>20</sup> Figure 5 shows the SPV behavior of a Cd-rich CdTe surface [curve (a)] before {same as Fig. 1 [curve (a)]} and [curve (b)] after etching by a 1%  $\text{Br}_2/\text{CH}_3\text{OH}$  solution. Clearly, the transition at  $E_1$  becomes stronger, while the transition at  $E_2$  practically disappears. Therefore, it seems reasonable to assign the  $E_1$  and  $E_2$  transitions to  $\text{TeO}_2$ -CdTe interaction and Cd atom displacement, respectively.

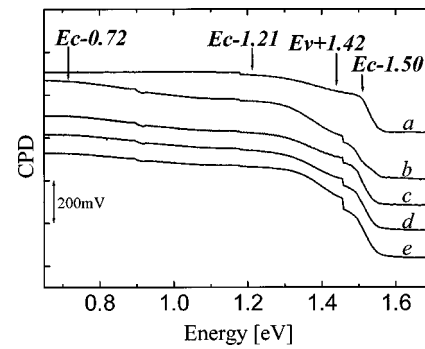


FIG. 6. SPV curves of Cd-rich surface of  $\text{Cd}_{0.937}\text{Zn}_{0.063}\text{Te}$  before and after different chemical etchings: (a) before etching; (b) etched by 1%  $\text{Br}_2/\text{CH}_3\text{OH}$  solution; (c) etched by HCl; (d) and (e) etched by 5 M KOH + 3.5 M NaCl solution at room temperature and 80 °C, respectively. The spectra are vertically shifted for clarity.

As mentioned earlier, the Cd-rich surface of the  $p$ -CdTe should have another surface state at 1.11 eV above the VBM associated with Cd atom displacement, which could not be observed at the  $n$ -CdTe surface. It is not clear whether the concentration of this state is too low to be detected, or whether it becomes a filled acceptor state in  $n$ -CdTe. In the latter case, the transition energy from such a state to the CBM is about 0.40 eV, which is beyond our spectral range.

Moving to Fig. 1 [curve (b)], a subband gap transition is obtained for the  $n$ -CdZnTe at 1.21 eV, with the same transition polarity as that of the  $E_1$  transition of CdTe. It has been reported that  $\text{TeO}_2$  is also present at CdZnTe surfaces.<sup>21</sup> This is true for our sample as shown later (insert in Fig. 7). By comparison to CdTe, the state at CBM-1.21 eV may be attributed to  $\text{TeO}_2$ -CdZnTe interaction. Another transition is found at 1.42 eV. This indicates a relatively weak transition from the VBM to an unoccupied donor. Similarly to the  $E_2$  transition in CdTe, this transition may be related to Cd atom displacement. The reason for the weaker transition in comparison with that in CdTe may reflect the effect of increasing bond energy and decreasing defect density due to the introduction of Zn to CdTe.<sup>4,22,23</sup>

Figure 6 shows the SPS results obtained after various chemical treatments of the CdZnTe sample. In comparison with the untreated surface [curve (a)],  $\text{Br}_2/\text{CH}_3\text{OH}$  etching [curve (b)] enhances the 1.21 eV transition signal. This may be attributed to the increased  $\text{TeO}_2$  layer thickness and thus the stronger contribution of the  $\text{TeO}_2$  surface state to the SPV. On the other hand, a subsequent HCl etching [curve (c)] weakens this transition due to the oxide layer removal by HCl.<sup>11</sup>

Comparing our results with the work of Burstein *et al.*,<sup>20</sup> the SPS again shows its advantage in contactless characterization of the polar surfaces of CdZnTe (which has a similar surface electronic structure to CdTe). The SPS finding of a reduction in the Cd surface displacement density by Zn introduction indicates a possible method for monitoring the displacement density in semiconductor alloys.

An interesting phenomenon is that the  $\text{Br}_2/\text{CH}_3\text{OH}$  etching causes a rather widely distributed, new transition at  $0.72 \pm 0.05$  eV. This transition did not disappear after further treatment with HCl. Since this effect does not occur at the

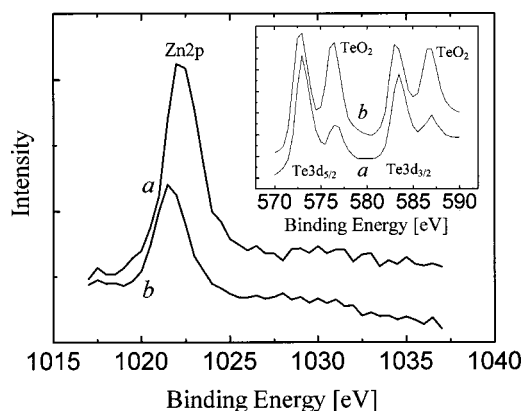


FIG. 7. XPS spectra of Zn 2p of  $\text{Cd}_{0.937}\text{Zn}_{0.063}\text{Te}$  (inset shows the Te 3d and  $\text{TeO}_2$  peak shapes) before (a) and after (b) chemical treatments in  $\text{KOH}+\text{NaCl}$  solutions.

$\text{Br}_2/\text{CH}_3\text{OH}$  treated CdTe surface, it seems not to be caused by a change in the surface concentrations of Cd, Te and/or their oxides. Since etching by  $\text{Br}_2/\text{CH}_3\text{OH}$  depletes the CdZnTe of Zn,<sup>21</sup> this transition may be associated with chemically induced Zn vacancies.

Treatments by  $\text{KOH}$  or  $\text{KOH}+\text{KCl}$  solutions can recover the stoichiometry of CdTe and CdMnTe etched by  $\text{Br}_2/\text{CH}_3\text{OH}$  and mineral acids.<sup>12</sup> Figure 7 shows the XPS Zn 2p peak [curve (a)] before and [curve (b)] after chemical treatment in  $\text{KOH}+\text{NaCl}$  solutions. The inset depicts the part of the spectrum showing the Te 3d and  $\text{TeO}_2$  peaks [curve (a)] before and [curve (b)] after the treatments. The analysis shows that the Zn surface concentration decreases by half after the treatments. Curves (d) and (e) in Fig. 6 show the SPV curves after treatments in  $\text{KOH}+\text{NaCl}$  solution at room temperature and  $80^\circ\text{C}$ , respectively [the SPV curve after treatment in  $\text{KOH}$  solution is similar to curve (d)]. The transition at 0.72 eV persists in agreement with its attribution to Zn vacancies.

#### IV. CONCLUSIONS

Using an experimentally improved band gap measurement methodology, surface photovoltage spectroscopy has been found to be an effective analytical tool for highly accurate determination of  $\text{Cd}_{1-x}\text{Zn}_x\text{Te}(111)$  alloy composition. The error in  $x$  is below 0.6%, which is comparable to the measurement results of a reference CdZnTe sample by conventional energy dispersive x-ray spectroscopy. Besides the CdZnTe(111) face, band gap and type, SPS enables investigation of the electronic structure of this sample: An acceptor

surface state has been found at 1.21 eV below the CBM and attributed to  $\text{TeO}_2$  species. A donor surface state has been found at  $\sim 1.42$  eV above the VBM with a lower concentration relative to CdTe and attributed to Cd atom displacement; a chemically induced surface state at 0.72 eV below the CBM may be due to Zn vacancies, as supported by XPS results.

#### ACKNOWLEDGMENTS

J. H. Y. is grateful to Tel Aviv University for a postdoctoral fellowship as well as to Dr. I. Shalish and other colleagues for their kind help in his postdoctoral program. Y. S. is grateful to Dinah and Henry Krongold for their generous support. The authors are grateful to Dr. L. Kronik for a critical reading of the manuscript.

- <sup>1</sup> *Semiconductors and Semimetals*, edited by R. K. Willardson and A. C. Beer (Academic, New York, 1978), Vol. 13.
- <sup>2</sup> *Semiconductors and Semimetals*, edited by T. E. Schlesinger and R. B. James (Academic, San Diego, 1995), Vol. 43.
- <sup>3</sup> Z. Q. Shi, C. M. Stahle, and P. Shu, *Proc. SPIE* **3553**, 90 (1998).
- <sup>4</sup> K. Guergouri, M. S. Ferah, R. Triboulet, and Y. Marfaing, *J. Cryst. Growth* **139**, 6 (1994).
- <sup>5</sup> S. P. Tobin *et al.*, *J. Electron. Mater.* **24**, 697 (1995).
- <sup>6</sup> L. Kronik and Y. Shapira, *Surf. Sci. Rep.* **37**, 1 (1999).
- <sup>7</sup> J.-P. Häring, J. G. Werthen, and R. H. Bube, *J. Vac. Sci. Technol. A* **1**, 1469 (1983).
- <sup>8</sup> M. Azoulay, M. A. George, A. Burger, W. E. Collins, and E. Silberman, *J. Vac. Sci. Technol. B* **11**, 148 (1993).
- <sup>9</sup> S. Sen, C. S. Liang, D. R. Rhiger, J. E. Stannard, and H. F. Arlinghaus, *J. Electron. Mater.* **25**, 1188 (1996).
- <sup>10</sup> P. D. Brown, K. Durose, G. J. Russell, and J. Woods, *J. Cryst. Growth* **101**, 211 (1990).
- <sup>11</sup> T. B. Wu, J. S. Chen, C. D. Chiang, Y. M. Pang, and S. J. Yang, *J. Appl. Phys.* **71**, 5212 (1992).
- <sup>12</sup> R. D. Feldman, R. L. Opila, and P. M. Bridenbaugh, *J. Vac. Sci. Technol. A* **3**, 1988 (1985).
- <sup>13</sup> A. Kalnitsky, S. Zukotynski, and S. Sumski, *J. Appl. Phys.* **52**, 4744 (1981).
- <sup>14</sup> A. Rohatgi, R. Sudharsanan, S. A. Ringel, P. V. Meyers, and C. H. Liu, *Proc. 20th IEEE Photovoltaic Specialists Conf.* (IEEE, New York, 1988), p. 1477.
- <sup>15</sup> L. Lassabatere, C. Alibert, J. Bonnet, and L. Soonckindt, *J. Phys. E* **9**, 773 (1976).
- <sup>16</sup> B. Adamowicz and J. Szuber, *Surf. Sci.* **247**, 94 (1991).
- <sup>17</sup> J. Lagowski, L. Jastrzebski, and G. W. Cullen, *J. Electrochem. Soc.* **128**, 2665 (1981).
- <sup>18</sup> L. Burstein, J. Bregman, and Y. Shapira, *Appl. Phys. Lett.* **57**, 2466 (1990).
- <sup>19</sup> L. Burstein, J. Bregman, and Y. Shapira, *J. Appl. Phys.* **69**, 2312 (1991).
- <sup>20</sup> L. Burstein, Y. Shapira, E. Moons, and D. Cahen, *Appl. Surf. Sci.* **74**, 201 (1994).
- <sup>21</sup> M. A. George, M. Azoulay, H. N. Jayathirtha, A. Burger, W. E. Collins, and E. Silberman, *Surf. Sci.* **296**, 231 (1993).
- <sup>22</sup> S. B. Qadri, E. F. Skelton, A. W. Webb, and J. Kennedy, *Appl. Phys. Lett.* **46**, 257 (1985).
- <sup>23</sup> A. Sher, A. Chen, W. E. Spicer, and C. K. Shih, *J. Vac. Sci. Technol. A* **3**, 105 (1985).